FINAL REPORT

Impact of Climate Change and Sea Level Rise on Stormwater Design and Reoccurring Flooding Problems in the Hampton Roads Region

Date: June 2016

Jonathan L. Goodall, PhD, PE, Associate Professor, University of Virginia
Venkataramana Sridhar, PhD, PE, Assistant Professor, Virginia Tech
with one postdoc, three graduate students, and five undergraduate students as co-authors

Prepared by:
University of Virginia
Department of Civil and Environmental Engineering
351 McCormick Rd, Thornton Hall
Charlottesville, VA 22904

Virginia Tech
Department of Biological Systems Engineering
155 Ag Quad Lane, Seitz Hall, RM 200
Blacksburg, VA 24061

1. Report No.	2. Government Accession No.	3. Recipient's Catalog No.

4. Title and Subtitle	5. Report Date
Impact of Climate Change and Sea Level Rise on Stormwater Design and Reoccurring Flooding Problems in the Hampton Roads Region	June 2016
	6. Performing Organization Code

7. Author(s):	8. Performing Organization Report No.
Jonathan L. Goodall, Venkataramana Sridhar, Jeffrey Sadler, Prasanth Valayamkunnath, Mirza Billah, Nicole Haselden, Kimberly Mellon, Allison Hackel, Veronica Son, Jordan Mayfield, and Mohamed Morsy	

9. Performing Organization Name and Address	10. Work Unit No. (TRAIS
University of Virginia Department of Civil and Environmental Engineering 351 McCormick Rd, Thornton Hall Charlottesville, VA 22904 Virginia Tech Department of Biological Systems Engineering 155 Ag Quad Lane, Seitz Hall, RM 200 Blacksburg, VA 24061	11. Contract or Grant No. DTRT13-G-UTC33

12. Sponsoring Agency Name and Address	13. Type of Report and Period Covered
US Department of Transportation Office of the Secretary-Research UTC Program, RDT-30 1200 New Jersey Ave., SE Washington, DC 20590	Final 7/1/15 – 6/30/16
	14. Sponsoring Agency Code

15. Supplementary Notes

16. Abstract

The information contained in this report is organized as three separate but related research studies. Collectively, these studies investigate the impact of climate change and sea level rise on transportation infrastructure within portions of the Hampton Roads region of Virginia. The first report "Impact of Sea Level Rise on Roadways in the Hampton Roads Region of Virginia" emphasizes the vulnerability of roadways to sea level rise in Norfolk and Virginia Beach. The second report "Impact of Climate Change on Design Rainfall Events in Hampton Roads, VA" explored various future precipitation scenarios in order to better understand climate change impacts to design rainfall events. The third report "Effect of rain gauge proximity on rain estimation for problematic urban coastal watersheds in Virginia Beach, VA" looks at the question of how rainfall variability within Virginia Beach impacts the ability to accurately measure rainfall using gauging stations. Each subreport is presented independently along with a title page listing the authors of that subreport. The University of Virginia completed the first and third subreports, while Virginia Tech completed the second subreport.

17. Key Words	18. Distribution Statement
Climate Change, Sea Level Rise, Reoccurring Flooding, Hampton Roads Region	No restrictions. This document is available from the National Technical Information Service, Springfield, VA 22161

19. Security Classif. (of this report)	20. Security Classif. (of this page)	21. No. of Pages	22. Price
Unclassified	Unclassified	46	

Executive Summary

The information contained in this report is organized as three separate but related research studies. Collectively, these studies investigate the impact of climate change and sea level rise on transportation infrastructure within portions of the Hampton Roads region of Virginia.

The first report "Impact of Sea Level Rise on Roadways in the Hampton Roads Region of Virginia" emphasizes the vulnerability of roadways to sea level rise in Norfolk and Virginia Beach. The research team used geospatial data and geographic information system (GIS) data processing techniques to estimate the roadways that would be vulnerable to flooding due to various sea level rise scenarios. The results are presented for two different events: 1) high tide conditions and 2) 100-yr storm surge conditions. The results of the study indicated that by 2100 with intermediate sea level rise predictions, more than 10% of major roadways will be inundated at high tide. Additionally, more than 70% of roadways will be inundated in the same sea level scenario during a 100 year storm surge event. The results of the study also make use of traffic count data in order to identify several critical roadways segments that are vulnerable to flooding with sea level rise scenarios over the next century. These roadways should be the focus of further studies to verify their flood risks and explore options for reducing these flood risks.

The second report "Impact of Climate Change on Design Rainfall Events in Hampton Roads, VA" explored various future precipitation scenarios in order to better understand climate change impacts to design rainfall events. Precipitation data from weather stations as well as from downscaled regional or global climate and weather models were analyzed for the Hampton Roads region. The precipitation modeling techniques were compared to actual precipitation data to determine the percent biased of each model. The percent biased could be used in the future to correct the model output data. The model, GFDL-ESM2M, which had one of the lowest percent biased was then used to model several climate change scenarios. The scenarios indicated increases in precipitation for much of the Hampton Roads district under the RCP4.5 scenario and for the entire region for the RCP8.5 scenario. The Eastern Shore is projected to have the lowest increase, while Suffolk is projected to have the highest increase.

The third report "Effect of rain gauge proximity on rain estimation for problematic urban coastal watersheds in Virginia Beach, VA" looks at the question of how rainfall variability within Virginia Beach impacts the ability to accurately measure rainfall using gauging stations. Available rain gauge networks were inventoried and rainfall observations at a 15 minute time step were gathered for the 20 days over a three year period with the highest rainfall totals. City officials assisted in identifying seven problem areas for flooding within Virginia Beach. A high-resolution digital elevation model (DEM) was used to derive watersheds for each of these problem areas. Experiments were conducted to better understand how local rainfall observations for each of the problem area watersheds impacted the ability to accurately predict the rainfall that fell on the watershed. The findings showed that having a gauge within 1km of the watershed greatly reduced the precipitation prediction error, especially for a 15 minute time step. This results suggest the need for a dense rainfall monitoring network for coastal cities like Virginia Beach where flooding risks are increasing due to sea level rise and climate change.

Following this Executive Summary, each subreport is presented independently along with a title page listing the authors of that subreport. The University of Virginia completed the first and third subreports, while Virginia Tech completed the second subreport.

Acknowledgements

The authors thank the City of Virginia Beach Public Works, the Hampton Roads Sanitation District, and Weather Underground for their data and assistance. Abby Blase assisted in preparing the report and Emily Parkany provided valuable feedback on the report.

Disclaimer

Impact of Sea Level Rise on Roadways in the Hampton Roads Region of Virginia

Jeffrey M. Sadler[a], Nicole Haselden[b], Kimberly Mellon[b], Allison Hackel[b], Veronica Son[b], Jordan Mayfield[b], Jonathan L. Goodall Ph.D., P.E.[c]

[a] *Graduate Research Assistant, Civil and Environmental Engineering, University of Virginia jms3fb@virginia.edu*
[b] *Undergraduate Student, Civil and Environmental Engineering, University of Virginia*
[c] *Associate Professor, Civil and Environmental Engineering, University of Virginia goodall@virginia.edu*

Contents

List of Figures

List of Tables

Problem

Globally, millions of people are affected by coastal flooding each year (Prime et al., 2015). Recent flooding events in the United States have caused significant social and economic damage to coastal cities. Hurricanes Katrina (Kates et al., 2006) and Sandy (Galarneau et al., 2013) in New Orleans, Louisiana and New York City, New York respectively, resulted in more than 1,500 fatalities and $100 billion in damage. As sea levels rise, flooding events in coastal cities are likely to occur more frequently and with greater severity (Nicholls and Cazenave, 2010). While the destruction caused by major storm events is well known, more frequent, but less severe floods, or 'nuisance floods,' are already disrupting transportation systems (Ezer and Atkinson, 2014). These smaller disruptions have a high cumulative economic and social cost to coastal cities and are increasing in frequency (Suarez et al., 2005; Sweet et al., 2014).

Flooding due to climate change is likely to significantly damage valuable transportation infrastructure systems (Kates et al., 2006; Meyer and Weigel, 2011). In the United States alone, transportation assets were valued at over $7 trillion in 2012, with over half of these assets being publically owned (U.S. Department of Transportation, 2013). An important first step in adapting to increased flood risk is to identify areas most vulnerable to flooding so that physical and economic resource spending can be prioritized (El Raey et al., 1999; Lambert et al., 2013; Roberts, 2010). Roads and bridges which a) are susceptible to flooding due to low elevations and b) have high traffic volumes are of special concern and, for the purposes of this paper, are referred to as critical road segments.

Prior studies have addressed the vulnerability of transportation networks to sea level rise. Oswald and Treat (2013) developed and applied a framework for modeling transit inundation using GIS data. Similarly, Bloetscher et al. (2014) used down-scaled elevation data, including high-resolution LiDAR data, to identify vulnerable transportation infrastructure. Instead of focusing on the physical infrastructure itself, Suarez et al. (2005) modeled flood impacts on a transportation system's performance using lost trips and delay times as measures of disruption.

Approach

This study adds to the current literature by combining high resolution elevation data with traffic data to produce detailed information of critical roadways in the Hampton Roads region of Virginia. Mitchell et al. (2013) and Kleinosky et al. (2006) performed studies of potential flooding effects on this region with a more general focus, rather than specifically considering transportation. Wu et al. (2013) focused on the combined impact of sea level rise and hurricanes on Hampton Roads transportation infrastructure. This study identifies not only vulnerable transportation infrastructure, but also the human impact this may have on in terms of travel disruptions. Wu et al. (2013) did examine the effects of sea level rise and storm surge on transportation infrastructure, however, they did not consider traffic volumes and only investigated the effects of extreme weather events, namely hurricanes, and not tidal-driven flooding impacts. Mitchell et al. (2013) identified areas prone to recurrent flooding in the Hampton Roads region, but it did not look further into the effect on transportation infrastructure in particular.

This study aims to predict the impact of sea level rise, mean high tide, and storm surge from a 100-year storm-surge event on Virginia Department of Transportation (VDOT) roads with known traffic volumes in Norfolk and Virginia Beach from the year 2000 to 2100. Norfolk and Virginia Beach were selected as a subset of the larger Hampton Roads region due to the population, important military interests, and tourist attractions in these cities.

Methodology

Study Area

Due to the its low-lying geography, Hampton Roads is the second most vulnerable area to sea level rise in the United States for its population and size, behind New Orleans (Fears, 2012). This region is the 34th most populous metropolitan area, with the 38th largest economy in the United States (hrp.org). It is home to the world's largest naval base, multiple universities, the NASA Langley Research center, and other valuable assets These attributes make the region valuable to a wide range of stakeholders, from its 1.7 million inhabitants to the U.S. Department of Defense (Kleinosky et al., 2006).

Roadway flood-risk analysis

To evaluate future sea level rise risks on transportation infrastructure in Virginia Beach and Norfolk, a geographic information system (GIS) was used to perform quantitative and visual analysis. In order for gravity-driven stormwater infrastructure to continue to work properly, there needs to be sufficient head gradient from the street level to the sea level (Grigg, 2012). If the stormwater infrastructure outlets are below sea level, the stormwater infrastructure will not function properly, stormwater will backup within the system, and those streets served by the stormwater infrastructure will flood. For this reason, this study assumed roadways below sea level to be inundated.

This study considered three different ways flood water elevation might vary over time: long term increases in mean sea level, tidal influences, and storm surge from a 100-year storm surge event. Two different flooding scenarios were considered in the study: (i) flooding due to mean high tide and (ii) flooding due to storm surge from a 100-year storm surge event that occurred during high tide. Superimposed on both of these scenarios were low, intermediate, and high long-term mean sea level rise projections. The methodology was divided into two primary objectives. The first objective of the analysis was to calculate the percent of roadway flooded over time for the two flooding scenarios. The second objective was to identify critical roadways vulnerable to flooding by considering both the roadway's elevation and the Average Annual Weekday Daily Traffic (AAWDT) for the roadway.

Descriptions of Analyzed Data

Transportation Infrastructure Data:

A dataset for Virginia roadways called "Annual Average Daily Traffic volumes with Vehicle Classification Data" was obtained from VDOT (http://www.virginiadot.org/info/ct-trafficcounts.asp). These data included interstate highway, arterial and primary routes data, and AAWDT for the entire state from the years 1985 to 2014. The dataset was clipped to the Hampton Road's boundary to extract information for only the region being studied.

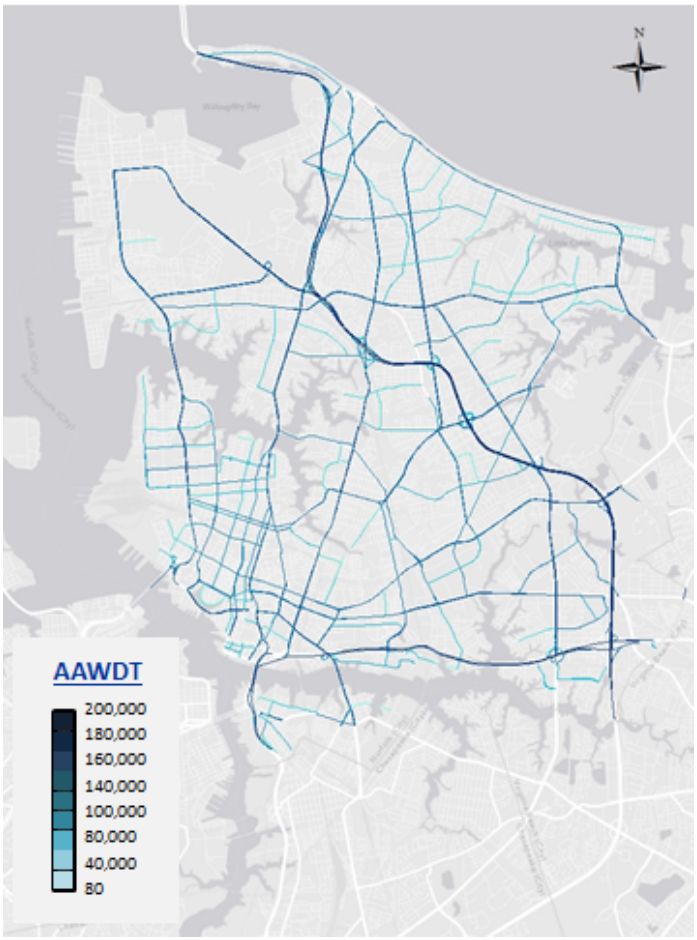

Figure 1. Norfolk AAWDT ranging from low traffic density (light blue) to high traffic density (navy blue) for the Norfolk region. *Source: Virginia Department of Transportation (VDOT).*

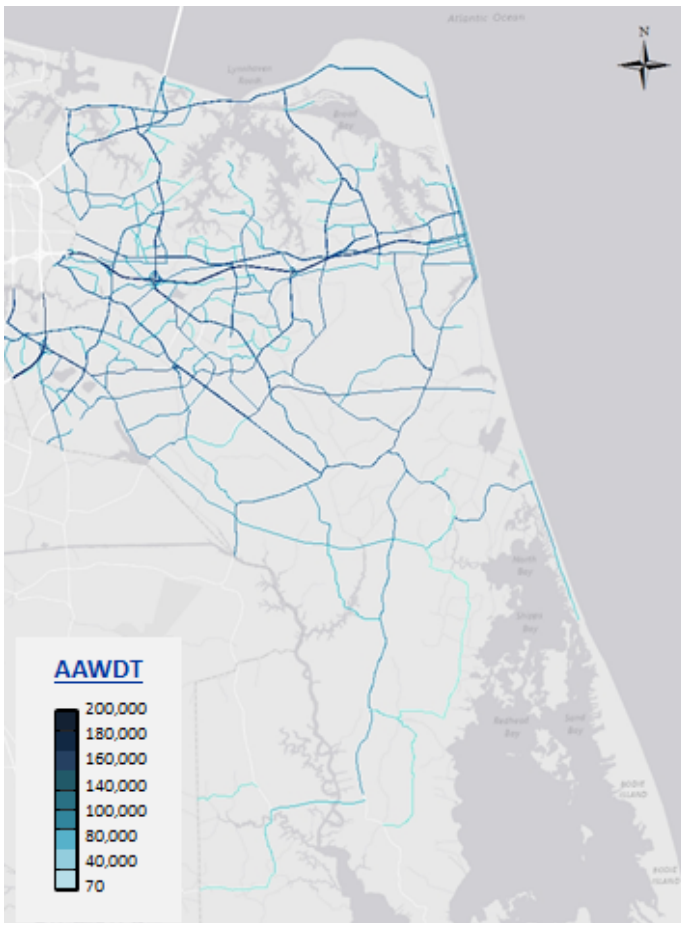

Figure 2. Virginia Beach AAWDT ranging from low traffic density (light blue) to high traffic density (navy blue) for the Virginia Beach region. Source: Virginia Department of Transportation (VDOT).

Figures 1 and 2 show the AAWDT for Norfolk and Virginia Beach, respectively. Both cities have high density roads located near the coast, many of which serve over 100,000 travelers daily.

Topographic Data:

A LiDAR digital elevation model (DEM), with a resolution of 0.76 meters (2.5 feet), was obtained from Virginia LiDAR (http://www.virginialidar.com). The DEM was used to estimate the elevations of roadway centerlines throughout the study area.

Storm Surge and Tide Data:

Annual exceedance probability levels and tidal data from Sewells Point Station, shown in Figure 3, were collected from the National Oceanic and Atmospheric Administration. The 1% exceedance probability value is the same as 100-year storm surge data used for this study. All data were adjusted to use the North American Vertical Datum of 1988 (NAVD88), for the year 2015.

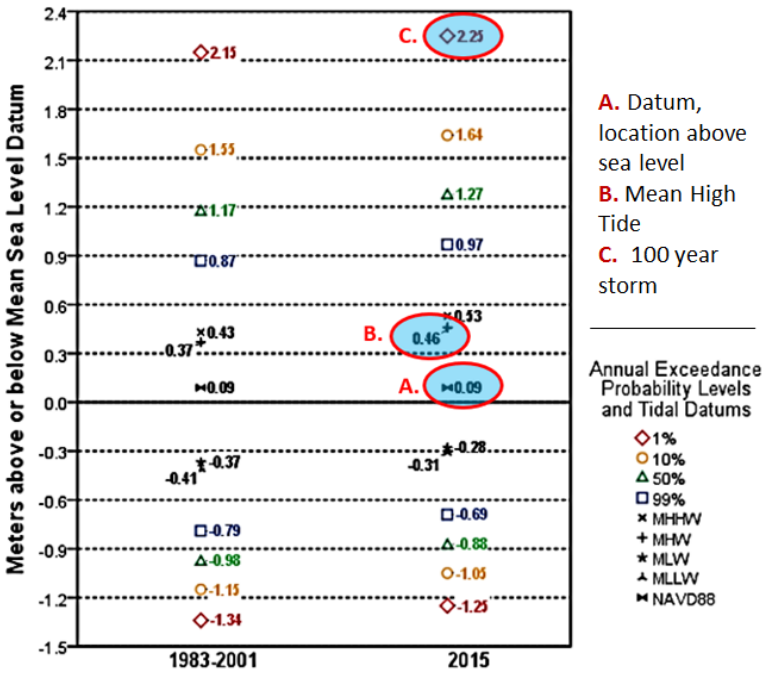

Figure 3. Annual Exceedance Probability Levels and Tidal Data from Sewells Point Station(National Oceanic and Atmospheric Administration, 2016)

Sea Level Rise Data:

Low, intermediate, and high sea level rise scenarios for Southeastern Virginia were obtained from the Virginia Institute of Marine Science (VIMS) (Figure 4). The low scenario represents historic rates of sea level rise and projections with no acceleration. This scenario was based on the International Panel on Climate Change 4th Assessment Model, which used conservative assumptions about future emissions and sea level rise. The intermediate scenario represents upper-end projections from semi-empirical models. The high scenario represents upper-end projections as well as sea level rise contributions from ice-sheet loss and glacial melting. Sea level rise in meters was predicted for the years 1992 through 2100 (Virginia Institute of Marine Science, 2014). These different models highlight the uncertainty in climate change predictions. The historic model predicts only 0.49 meters of sea level rise by 2100, while the high scenario predicts 2.3 meters of sea level rise by the end of the century.

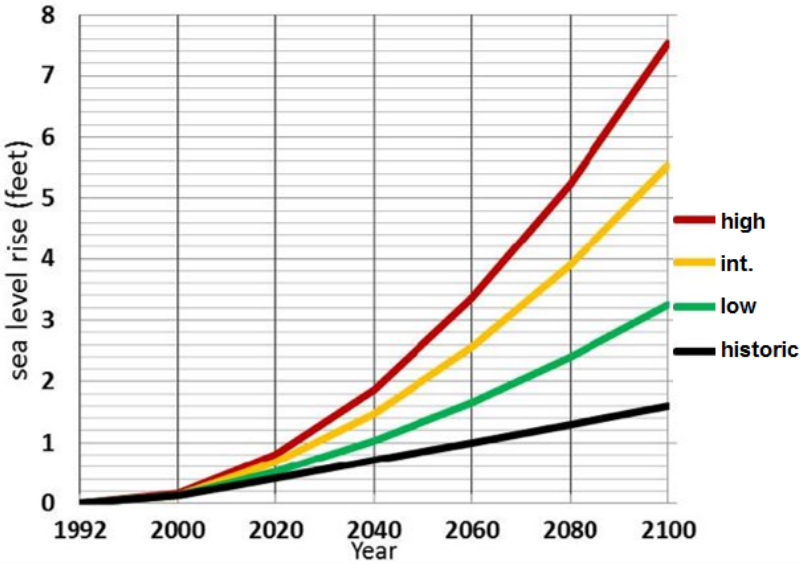

Figure 4. Sea Level Rise Scenarios for Southeastern Virginia (Mitchell et al., 2013)

Using the low, intermediate, and high sea level rise quantities shown in Figure 4, the values for the two flooding scenarios were calculated: (i) a combination of sea level rise and mean high tide and (ii) a combination of sea level rise, mean high tide, and storm surge from a 100-year storm surge event. Table 1 charts the values calculated for the intermediate sea level rise scenarios and the range for low to high sea level rise values for each year. These values were used to project flooded roadways over time as described in the subsequent section.

Table 1. Predicted Degree of Flooding Above NAVD88 Over Time

Year	Intermediate SLR + tide (meters)	Range (meters)	Intermediate SLR + tide + storm surge (meters)	Range (meters)
2000	0.61	0.00	2.96	0.00
2020	0.76	0.09	3.11	0.09
2040	1.01	0.24	3.35	0.24
2060	1.31	0.55	3.66	0.55
2080	1.74	0.85	4.08	0.85
2100	2.23	1.31	4.57	1.31

Projection of Flooded Roadway over Time

The effect of sea level rise, mean high tide, and storm surge on VDOT roadways was quantified by calculating the percent of roadway that would be inundated due to various sea level rise, tidal, and storm surge scenarios. For the first scenario, using data from Figures 3 and 4, the sea level rise and tidal elevation data were identified and summed to calculate the predicted elevation of the roadways susceptible to flooding for each year. This scenario represents tidal-driven, recurrent flooding (1).

$$FWE_i = SLR_i + (MHT + DA) \quad \textbf{(1)}$$

$FWE_i =$ flood water elevation for ith year (meters)
$SLR_i =$ sea level rise for year i (meters)
MHT = mean high tide = 0.46 meters
DA = NAVD88 adjustment = 0.09 meters

For the second scenario, the storm surge from a 100-year storm surge event was included in addition to sea level rise and mean high tide (2). This scenario represented "worst case" flooding due to a 100-year storm surge event occurring during high tide.

$$FWE_i = SLR_i + (MHT + DA) + (SS_{100-year} + DA) \quad \textbf{(2)}$$

$SS_{100-yr} =$ 100-year storm surge event = 2.25 meters

Once flood water elevations were determined, they were compared to the LiDAR topographic dataset was to determine the percent of VDOT roadways that would be affected by the sea level rise, tidal, and flooding scenarios until the year 2100.

Traffic Vulnerability

To identify critical roadways, AAWDT (Figures 1 and 2) was mapped along with road elevation for VDOT roads in Norfolk and Virginia Beach (Figure 5) to determine how many travelers will be impacted by the various flooding elevation scenarios. Three vulnerability levels were identified: (i) roads with low elevation (<3 m) and low traffic (<30,000 AAWDT), (ii) roads with low elevation (<3 m) and medium traffic (30,000<AAWDT<75,000), and (iii) roads with low elevation (<3 m) and high traffic (>75,000 AAWDT).

Findings

The results show the large amount of low-lying Virginia Department of Transportation (VDOT) roadways in Norfolk and Virginia Beach (Figure 5). Approximately 50% of the heavily-traveled roads only reach an elevation of about 3.7 meters. By 2020, current projections suggest that the combined effects of sea level rise, high tide, and storm surge from a 100-year storm surge event would result in these roads being completely inundated (Table 1).

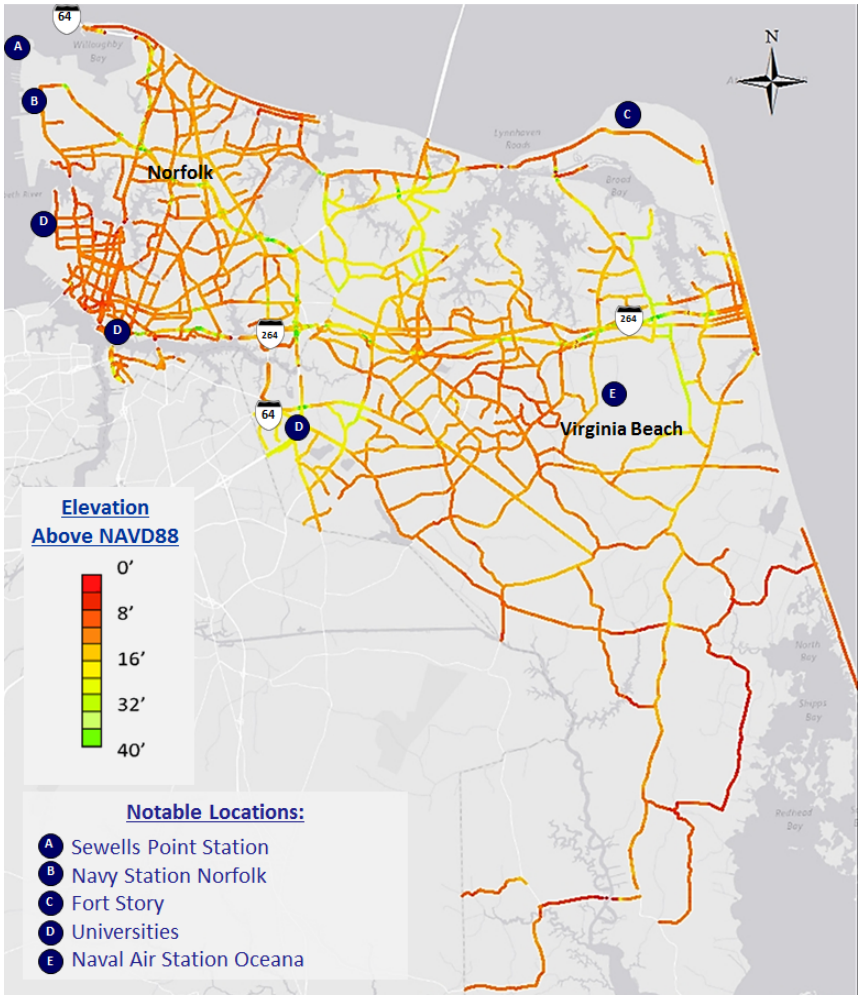

Figure 5. Transportation Infrastructure VDOT roadway elevations ranging from higher elevations (green) to lower elevations (red) for Norfolk and Virginia Beach. Source: Virginia Department of Transportation (VDOT), Virginia LiDAR.

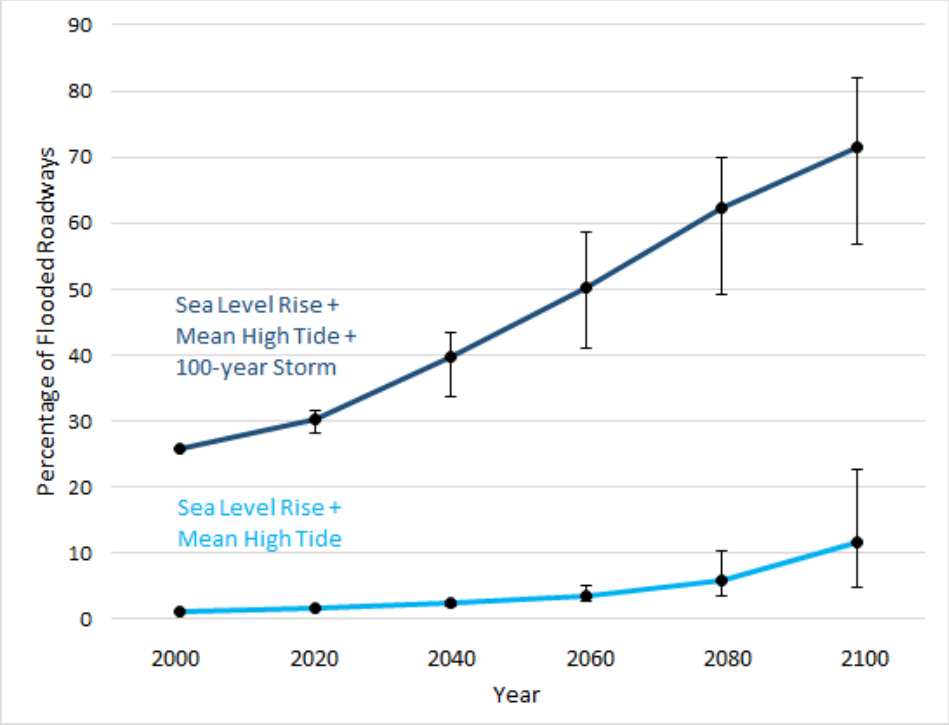

Figure 6. Projection of Flooded Roadways Over Time

Figure 6 shows the effect that flooding will have on roadways in the study region over time. The "Sea Level Rise + Mean High Tide" line represents the tidal-driven, recurrent flooding scenario. The error bars on the line indicate uncertainty introduced by the different sea level rise scenarios. The results suggest that, by 2100 and under the high sea level rise projections, approximately 20% of VDOT roadways will be inundated as a result of mean high tide and sea level rise. Under the intermediate sea level rise scenario, approximately 10% of VDOT roadways will be inundated as a result of mean high tide and sea level rise. By 2060, projections suggest that approximately 4% of VDOT roadways will be inundated due to mean high tide and an intermediate sea level rise scenario.

The "Sea Level Rise + Mean High Tide + 100-year Storm" line in Figure 6 represents a scenario with the combined effects of sea level rise, mean high tide, and a 100-year storm surge. Results suggest that, by 2100, this scenario will result in over 80% of VDOT roadways being inundated under the "worst case" sea level rise conditions. Under intermediate sea level rise conditions, still more than 70% of VDOT roads will be inundated. By 2060, projections suggest that between 40% and 60% of VDOT roadways will be inundated due to mean high tide, sea level rise, and storm surge.

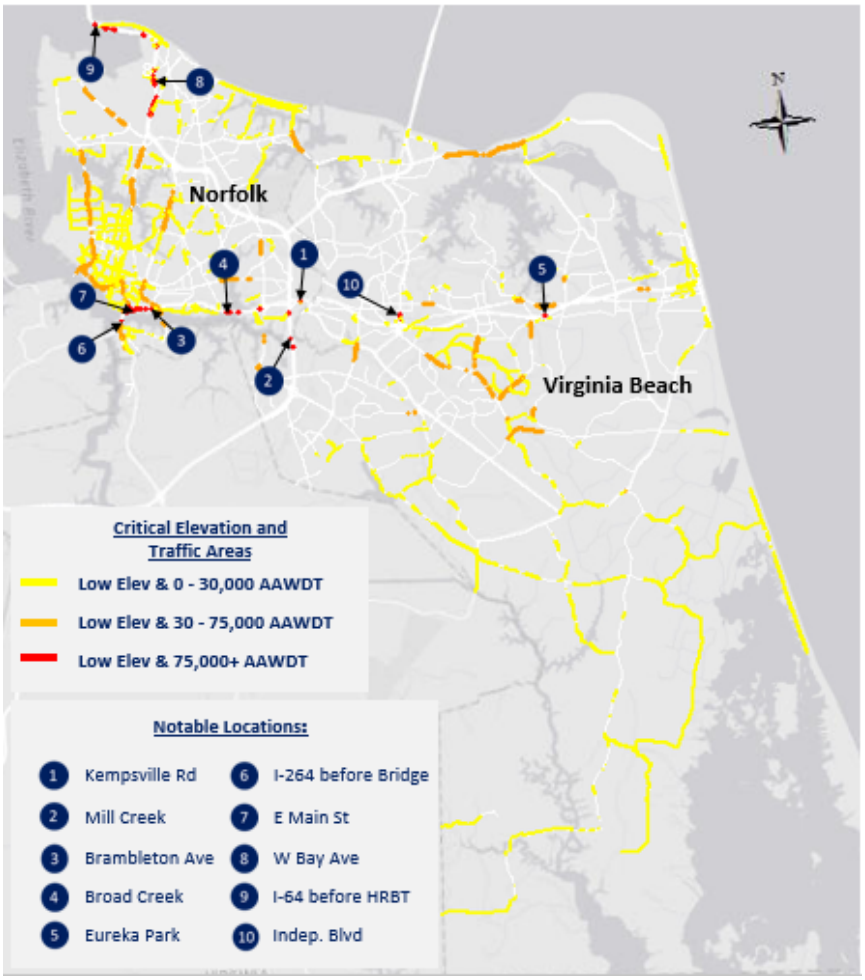

Figure 7. Identification of Critical Elevation and High Traffic DensityLow elevation VDOT roadways (below 3.04 meters) are categorized based on AAWDT. Source: Virginia Department of Transportation (VDOT), Virginia LiDAR.

Figure 7 shows the identified critical roadways in the study area with ten notable locations highlighted. Bridges were excluded from the analysis, as a "bare-earth" digital elevation model was used, where bridge elevations are set below zero. The ten critical locations were compared in terms of the predicted time when the roadways would be inundated from (i) sea level rise and mean high tide (SLR + Tide) and (ii) sea level rise, mean high tide, and a 100-year storm surge event (SLR + Tide + SS) (Table 2).

Table 2. Comparison of Elevation to AAWDT Considering Critical Locations

Point	Location	City	Elevation above NAVD88 (meters)	Year of Complete Inundation SLR + Tide	Year of Complete Inundation SLR + Tide + SS	AAWDT
1	Intersection of I-264 and Kempsville Road	Norfolk	2.9	> 2100	Present	198,000
2	I-64 near Mill Creek	Norfolk	1.9	2100	Present	146,000
3	Intersection of I-264 and Brambleton Avenue	Norfolk	2.0	2100	Present	131,000
4	Intersection of I-264 and Broad Creek	Norfolk	1.5	2080	Present	123,000
5	I-264 near Eureka Park	Virginia Beach	1.7	2080	Present	111,000
6	I-264 Connection South of Berkley Bridge	Norfolk	1.1	2060	Present	107,000
7	Intersection of I-264 and E Main Street	Norfolk	3.0	> 2100	2020	105,000
8	Intersection of I-64 and W Bay Avenue	Norfolk	2.3	> 2100	Present	93,000
9	I-64 W before Hampton Roads Bridge Tunnel	Norfolk	2.2	2100	Present	88,000
10	Intersection of Independence Boulevard and Garrett Drive	Virginia Beach	2.6	> 2100	Present	76,000

The results suggest that all ten locations will be inundated due to the combined effects of sea level rise, mean high tide, and storm surge by the year 2020, with nine out of the ten locations already vulnerable to flooding under these conditions. Six of the ten locations also face recurrent flooding from sea level rise and mean high tide by the end of the century, with one location beginning by 2060, two more by 2080, and three more by 2100. Inundation of these roadway sections, given their high traffic volume, could represent significant challenges for the region. Efforts to raise roadways with low elevation and high traffic in coming years will be important to avoid travel disruptions due to recurrent, tidal-driven flooding.

Limitations of Study

This study assumed that all roads with low elevations would be vulnerable to flooding when sea level rises above that roadway's elevation. In reality, hydrologic connectivity in the region would mean that roads further inland may be protected against flooding due to high tides. These roads may still be impacted by rising

sea levels due to the associated rise in groundwater tables; however, they will be less susceptible to tidal-driven flooding. Future research should investigate hydrologic connectivity in the region and its role in tidally-driven flooding of transportation infrastructure.

The study also assumed that tide levels and storm surge from a 100-year storm surge event will be constant as sea levels rise, which may not hold true. Future research should explore the potential variability in storm surge and tides as sea levels rise. More sophisticated approaches using hydrodynamic models capable of projecting how inland flooding due to storm surge will impact transportation infrastructure would also provide more accurate assessments of transportation vulnerability due to extreme events. The hydrodynamics of flooding due to storm surge are complex and this work is meant as a first approximation of vulnerable road infrastructure that could be improved with more detailed hydrodynamic modeling efforts.

Even with the assumption of constant storm surge and tidal variance, there is significant uncertainty in the sea level rise predictions themselves. Three different scenarios were chosen to represent low, intermediate and high predictions of sea level rise in this study to capture this uncertainty. More recent literature on sea level rise has suggested that the actual sea level rise may be much higher than previously thought due to various factors, including instability of the Antarctic ice sheet. These factors may cause an additional meter of sea level rise by the end of the century and up to 15 meters by 2500, nearly doubling prior sea level rise projections (DeConto and Pollard, 2016). The uncertainty about sea level rise is a challenging problem for long-term planning. Researchers are still advancing knowledge of sea level rise, and it will be critical for planners to adjust to new predictions, as the science continues to advance. For this reason, simple elevation-based data of transportation assets may be an effective way for planning for future sea-level rise vulnerability given these uncertainties.

Conclusions

The objectives of this research were to (i) quantify the impacts of sea level rise, mean high tide, and a 100-year storm surge event on roadways in Virginia Beach and Norfolk; and (ii) identify critical roadway sections within Norfolk and Virginia Beach. Under the immediate sea level rise scenario 2060, approximately 4% of major roads in Virginia Beach and Norfolk are predicted to be regularly flooded due to sea level rise and mean high tide. This increases to over 50% of major roads with the addition of a 100-year storm surge. Given a high sea level rise scenario, by 2100, more 20% of major roads are predicted to be regularly flooded due to sea level rise and mean high tide; this increases to over 80% of major roads with the addition of storm surge.

Using AAWDT data from VDOT, the most critical roadway sections, meaning those with both low elevations and high daily traffic volumes, were identified. Ten sections of roadways in Virginia Beach and Norfolk were identified as high traffic roadways (AAWDT > 75,000) and low-lying (elevation < 3 m), making them at-risk for flooding due to sea level rise, mean high tide, and storm surge from a 100-year storm surge event. Results suggest that nearly all of these road segments are vulnerable to flooding from extreme events now (9 out of 10) and all will be vulnerable to flooding from an extreme event by 2020. One of the locations will be vulnerable to flooding from high tide events by 2060, two by 2080, and three more by 2100. The results suggest that these locations should be high priority areas for infrastructure investments to minimize traffic disruptions due to recurrent, tidal-driven flooding.

Although this study focused on the two cities in the Hampton Roads region of Virginia, in a similar way, the methodology could be applied to other coastal areas to identify vulnerable roadway sections. Secondly, this study could easily be integrated into a method like the Climate Change Adaptation Tool for Transportation: Mid-Atlantic framework (Oswald and McNeil, 2013) to provide municipalities with not only a list of at-risk areas of roadway, but also a path forward to plan for future adaptation efforts.

Recommendations

The results of this study identify at-risk roadways in Virginia Beach and Norfolk. Specific locations with low elevation and high traffic volumes were highlighted. It is recommended that all at-risk roadways and especially those identified with high traffic volumes be considered when prioritizing flood mitigation efforts.

The results suggest that efforts to reduce flood risk at these locations will be important in minimizing travel disruptions due to recurrent, tidal-driven flooding.

Impact of Climate Change on Design Rainfall Events in Hampton Roads, Virginia

Prasanth Valayamkunnath[a], Mirza Billah, Ph.D.[b], Venkataramana Sridhar, Ph.D., P.E.[c]

[a] *Graduate Research Assistant, Biological Systems Engineering, Virginia Tech*
[b] *Postdoctoral Scholar, Biological Systems Engineering, Virginia Tech,*
[c] *Assistant Professor, Biological Systems Engineering, Virginia Tech, vsri@vt.edu*

Contents

List of Figures

List of Tables

Problem

Precipitation events of large magnitude often disrupt the normal activities through disastrous flooding in the urban areas. This research addresses two needs put forth by stakeholders in the Hampton Roads region. The first need is to update design storms used to design stormwater infrastructure in order to better account for climate change impacts. The second need is to better account for the impact of reoccurring flooding due to sea level rise on transportation project prioritizations. The frequency and magnitude of the large precipitation events are increasing and are expected to be intensified in the coming future due to climate change (Karl and Knight, 1998; Osborn et al., 2000; Sen Roy and Balling, 2004; Solomon et al., 2007, Min et al., 2011). Climate change is expected to impact severely at urban locations as these locations are the center of human activities. The built infrastructure to facilitate human activities are in jeopardy, susceptible to flooding and associated damages.

The geographic location of Hampton Roads, Norfolk and Virginia Beach metropolitan region along the Chesapeake Bay and the Atlantic Ocean makes them extremely vulnerable to urban and coastal flooding (Figure 1). The urban areas in southeastern Virginia experience an average of 1200 mm precipitation each year. The record shows a below average precipitation at Norfolk and Hampton Roads, while, an above average precipitation at Suffolk and Williamsburg. Within the city limits, the precipitation in the form of rainfall frequently exceeds the ability of the land to retain and/or safely discharge them into the ocean. The current design of the drainage infrastructure is unable to manage water in the urban system that results in a temporary road closure to the loss of homes, property and life. Therefore, there is a prime interest of redeveloping design storm to accommodate future climate condition in the planning tool for the urban drainage system of southeastern Virginia for the proper management of the flooding occurrences.

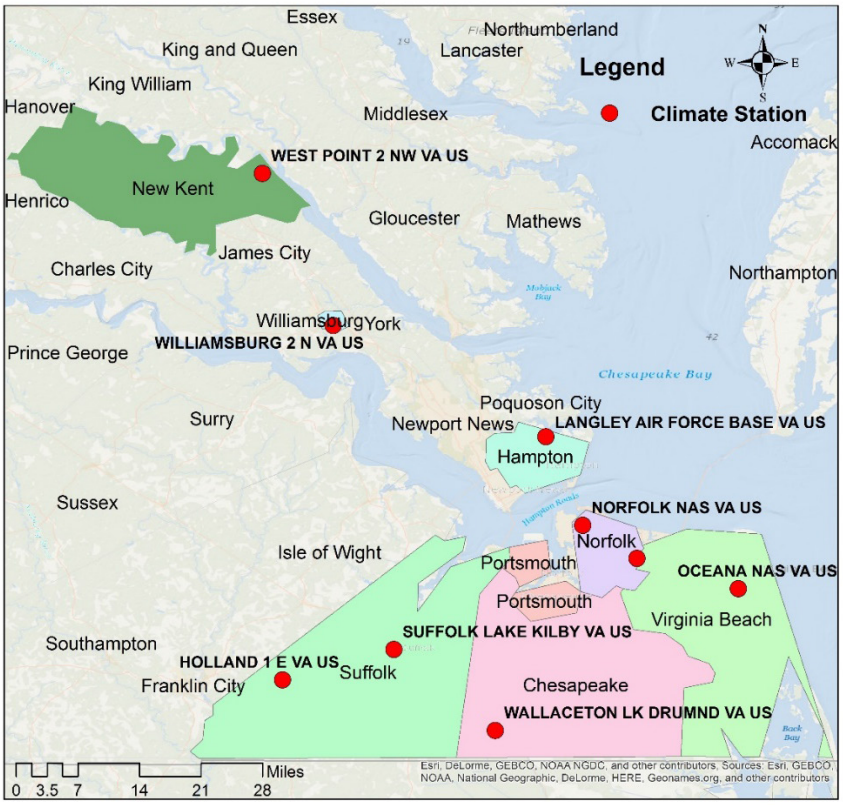

Figure 1: Spatial map of the meteorological stations of the GHCND in the southeastern Virginia. The GHCND observation at Langley Air Force Base is considered for Hampton region precipitation analysis.

Approach

Both meteorological records and downscaled gridded estimates are collected or generated to provide annual maximum precipitation in southeastern Virginia. The daily precipitation records are collected from 9 (nine) stations based on the long-term availability of data from National Climatic Data Center (NCDC) and 2 (two) of these stations are also considered for sub-daily precipitation records. These stations are listed in Table 1. The gridded daily estimates of precipitation over the study region are (i) extracted for the daily downscaled precipitation from 15 climate models (Table 2), (ii) simulated for the hourly downscaled precipitation using Weather Research and Forecasting (WRF) model. Both extracted and simulated precipitation estimates have the same $1/16^{th}$ (~ 4 km) of a degree spatial resolution. These gridded precipitation estimates are used to provide both temporal variation and spatial distribution of the annual maximum events over southeastern Virginia.

Table 1: List of the in-situ observation station of the Global Historical Climatology Network (GHCND) for precipitation trend analysis for the period of 1950~2010 over southeastern Virginia. The italic indicates the stations considered for also sub-daily precipitation records.

Station	Name of the stations	Elevation	Latitude	Longitude
Holland	Holland 1 E VA US	0	36.6833	-76.7833
Suffolk	Suffolk Lake Kilby VA US	0	36.7333	-76.6000
Wallaceton	Wallaceton Lake Drummond VA US	0	36.6000	-76.4333
West Point	West point 2 NW VA US	0	37.5167	-76.8167
Williamsburg	*Williamsburg 2 N VA US*	*21*	*37.2667*	*-76.7000*
Hampton	Langley Air Force base VA US	3	37.0833	-76.3500
Norfolk Airport	*Norfolk International Airport VA US*	*0*	*36.8833*	*-76.2000*
Norfolk	Norfolk NAS VA US	0	36.9375	-76.2893
Oceana	Oceana NAS VA US	7	36.8333	-76.0333

The extracted precipitation from the climate models are the downscaled estimates that applied Multivariate Adaptive Constructed Analogs (MACA) technique (Abatzoglou, 2013). These data are available for CONUS and requires transformation before use. These daily precipitation datasets are available for the period of 1950-2099 that are useful to evaluate the performance of the models to capture historical period (1950-2005) in comparison with observations, while precipitation estimates for the period of 2016-2099 can be used for future prediction. The grid cells corresponding to the location of the NCDC observations are used for evaluation of precipitation estimates. The performance is measured in terms of percent bias that is calculated from the deviation of the annual daily maximum precipitation for corresponding models and locations. These bias can be incorporated in the future precipitation estimates in the corresponding models and locations to reduce the uncertainty in the future precipitation characteristics for the period of 2016-2099 with two Representative Concentration Pathways (RCPs) scenarios, namely RCP4.5 and RCP8.5.

The simulated hourly precipitation is generated from WRF model with a spatial resolution of $1/16^{th}$ of a degree similar to the extracted climate precipitation resolution. These sub-daily precipitation are generated for the period of 1985-2010 and are used to evaluate the performance of the WRF model to capture annual hourly maximum precipitation event for the period of 1985-2010. The grid cells corresponding to the location of the NCDC observations are used for evaluation of hourly precipitation events. The performance is measured in terms of percent bias at 2 locations in the study regions. The calculated bias is applied to the corresponding locations and surrounding grid cell to generate bias corrected hourly precipitation estimates.

Table 2: List of the climate models of the Coupled Model Intercomparison Project 5 (CMIP5) that are downscaled using Multivariate Adaptive Constructed Analogs (MACA) techniques for precipitation trend analysis for the period of 1950~2099.

Model	Model Country	Model Agency
BCC-CSM1-1	China	Beijing Climate Center, China Meteorological Administration
BCC_CSM1-1-m	China	Beijing Climate Center, China Meteorological Administration
BNU-ESM	China	College of Global Change and Earth System Science, Beijing Normal University, China
CanESM2	Canada	Canadian Centre for Climate Modeling and Analysis
CCSM4	USA	National Center of Atmospheric Research, USA
CNRM-CM5	France	National Centre of Meteorological Research, France
CSIRO-Mk3-6-0	Australia	Commonwealth Scientific and Industrial Research Organization/Queensland Climate Change Centre of Excellence, Australia
GFDL-ESM2M	USA	NOAA Geophysical Fluid Dynamics Laboratory, USA
GFDL-ESM2G	USA	NOAA Geophysical Fluid Dynamics Laboratory, USA
INM-CM4	Russia	Institute for Numerical Mathematics, Russia
IPSL-CM5A-LR	France	Institut Pierre Simon Laplace, France
IPSL-CM5A-MR	France	Institut Pierre Simon Laplace, France
IPSL-CM5B-LR	France	Institut Pierre Simon Laplace, France
MIROC5	Japan	Atmosphere and Ocean Research Institute (The University of Tokyo), National Institute for Environmental Studies, and Japan Agency for Marine-Earth Science and Technology
MIROC-ESM	Japan	Japan Agency for Marine-Earth Science and Technology, Atmosphere and Ocean Research Institute (The University of Tokyo), and National Institute for Environmental Studies

Methodology

Meteorological Observations

The collection of the daily and hourly precipitation data started with downloading daily precipitation records from NCDC for 9 locations for the period of 1950~2010. The quality of the data is controlled using quality assurance reviews, including checks for spurious changes in the mean and variance and neighbor checks that identify outliers from both a serial and a spatial perspective.

CMIP5 Precipitation Data

The climate models-based daily precipitation are collected and transformed into ascii format for each grid cells of spatial resolution of $1/16^{th}$ of a degree. This high-resolution precipitation estimates are used to capture historical precipitation events at 9 locations of the meteorological station in the study region with 15 models for the period of 1950-2005. For the future period of 2016-2099, the daily precipitation of 15 models is also collected and transformed for 9 locations for temporal analysis. The climate models are also used for spatial distribution analysis for the study region of 16 x 16 grids cells that covers latitude of 36.5° to 37.5° and longitude of -75.8° to -76.9° in southeastern Virginia. These 256 cells from each climate model contain daily precipitation estimates for the period of 1950-2099 consisting of both historical and future precipitation analysis.

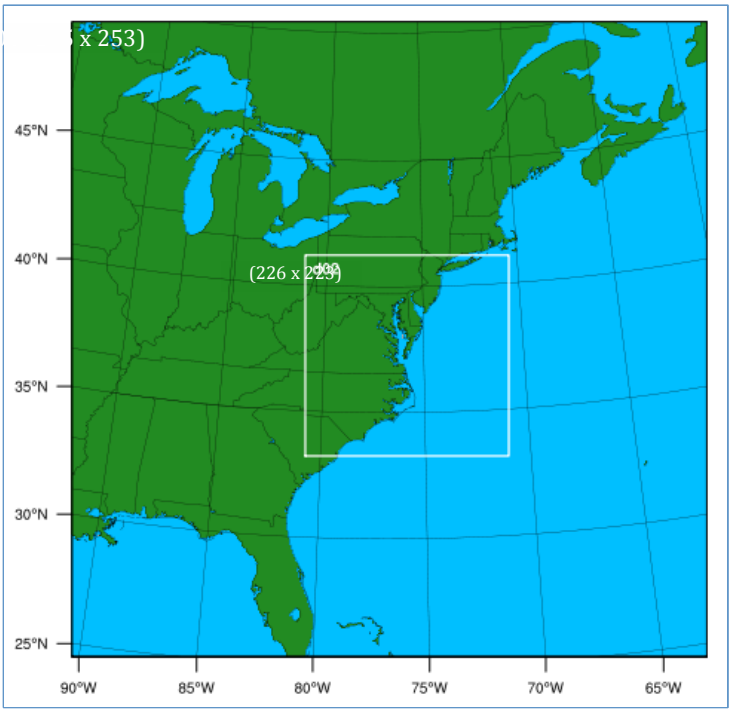

Figure 2: WRF model domain shows with the inner domain focusing on the study area.

WRF Precipitation Data

This study has also engaged WRF model with Advanced Research WRF (ARW) version 3.6.1 (Skamarock and Klemp, 2008) to dynamically downscale the regional climate with North American Regional Reanalysis data. This study consists a nested domain centered at 37.916 N and 76.721W. The parent domain contains 235 x 235 grid points with 12 km resolution and nested domain contains 226 x 223 grid points with $1/16^{th}$ of a degree (4 km) resolution. Both domains include 40 terrain following levels covering most of the Eastern United States (Figure 2). The inner domain was centered over the Hampton Roads region as it is the focal area for this particular study. The model uses MODIS-derived 20 category land cover and soil texture at 30 arc second resolution. The WRF model is adopted two-way nested domain with two domains to convert the coarse resolution of NARR (32 km) data to high-resolution WRF domain data ($1/16^{th}$ of a degree). The WRF model is simulated for the period of 1985 to 2010 and uses adaptive time step option to minimize processing time in the Advanced Research Computing (ARC) at Virginia Tech.

Bias Correction of WRF Precipitation with NCDC observations

The uncertainty generated in the downscaled precipitation of the model are estimated in terms of percent bias using hourly observation from NCDC stations at two locations (Table 1, *Italic*). A quantile–quantile adjustment is applied to the simulated precipitation estimates for correction to the downscaled precipitation from WRF model (Wood et al. 2004; Reichle and Koster 2004; Amengual et al., 2012). The quantile–quantile mapping transformation consists of calculating the changes quantile by quantile in the Cumulative Distribution Function (CDF) of hourly precipitation between 1985-2010 period using *in-situ* observation and WRF-based precipitation.

Findings

Annual Daily Maximum Precipitation

Figure 3 demonstrates the annual daily maximum precipitation trend using daily *in-situ* observations at the Hampton Roads region. On average, the precipitation trend in the Hampton Roads region shows a decreasing rate by mm/time. Likewise, these estimates of annual daily maximum precipitation facilitate detecting trend for other individual grid cells. Similar analysis was done for all of the stations.

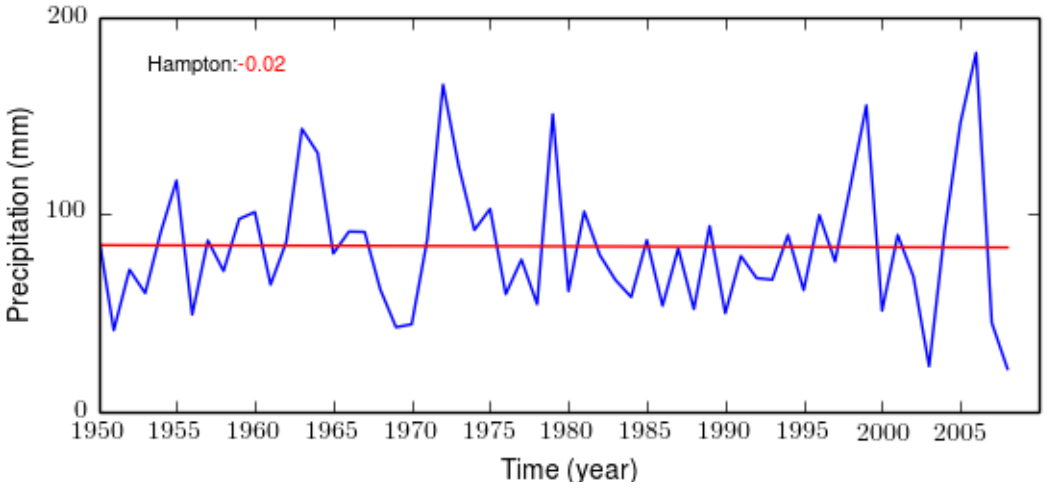

Figure 3: Variability in the annual daily maximum precipitation over the historical period of 1950-2010 at Hampton (Blue line; red line shows the annual trends). The bar represents average annual daily estimates of precipitation of largest 5 events.

Comparison of Annual Daily Maximum Precipitation between Observation & CMIP5-MACA-based Estimates

The comparison of *in-situ* daily observation of annual daily maximum precipitation provides the basis for estimating uncertainty generated by the model. Figure 4 shows such a comparison among the historical observation, maximum, and minimum estimates of annual daily maximum precipitation by the 15 climate models (shaded area) for Hampton region. The temporal variation of precipitation of all the models remains within this area. For any individual model, the comparison thus provides the percent bias that is captured at certain locations.

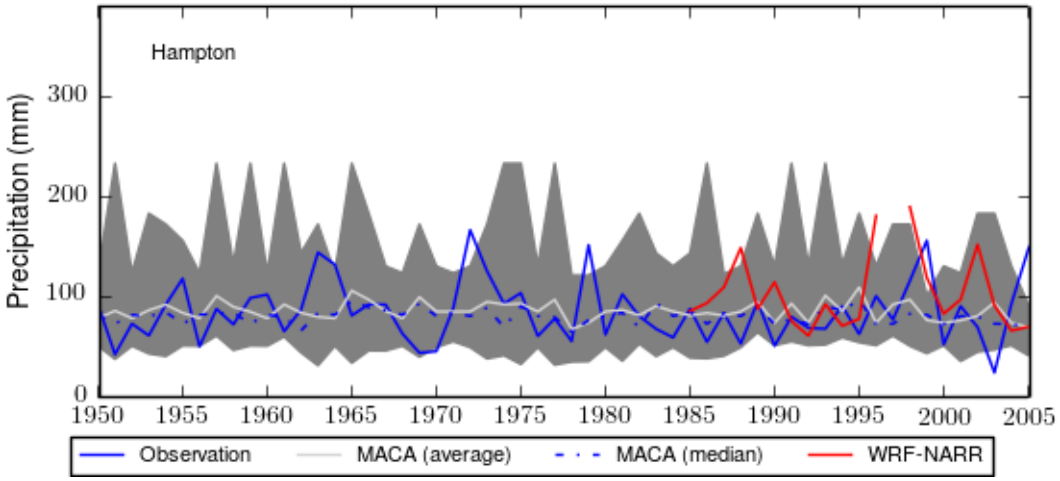

Figure 4: Variability in the annual daily maximum precipitation between observation and CMIP5-MACA based simulation over the historical period of 1950-2005 at Hampton. The shaded area represents the uncertainty produced by the MACA-downscaled estimates.

Percent Bias Estimates of the Climate Models

The computation of the percent bias for each 9 locations for 15 climate models is shown in Table 3. The matrix when evaluated for each model, demonstrates in favor of GFDL-ESM2M and BCC-CSM1-1-m models and compute the average percent bias of 10.6 and 11.6, respectively in the study region. These estimates are moderate for some models like BNU-ESM, CanESM2, CNRM-CM5, INM-CM4, IPSL-CM5A-LR, and IPSL-

CM5A-MR. The rest of the models show high percent bias corresponding to others. Location-wise, the Hampton (Langley) region shows the lowest bias when biases are considered from all 15 models. This estimate of percent bias provides an opportunity to estimate uncertainty in the annual daily maximum precipitation for both models and locations.

Table 3: Estimates of the percent bias (%) of the precipitation annual daily maximum precipitation of the climate models at 9 (nine) locations for the period of 1950~2005.

Models	Holland	Suffolk	Wallaceton	West Point	Williamsburg	Hampton (Langley)	Norfolk Airport	Norfolk	Oceana	Average
BCC-CSM1-1	35.9	2.1	24.6	26.8	13.7	0.3	11.7	18.3	12.7	16.2
BCC_CSM1-1-m	29.5	0.3	34.2	14.4	1.5	3.6	3.7	7.8	9.0	11.6
BNU-ESM	25.8	2.1	33.5	10.6	3.4	2.6	12.2	16.4	17.6	13.8
CanESM2	26.0	3.1	24.4	15.6	13.9	0.1	16.2	21.2	19.4	15.5
CCSM4	43.6	1.6	45.1	30.6	22.9	5.7	15.3	20.4	24.7	23.3
CNRM-CM5	36.9	11.0	29.6	24.6	12.8	4.4	6.9	11.0	14.4	16.8
CSIRO-Mk3-6-0	33.6	0.4	32.4	27.8	16.4	7.4	15.7	20.6	17.8	19.1
GFDL-ESM2G	29.6	2.5	29.1	39.7	6.7	0.2	14.4	20.7	22.8	18.4
GFDL-ESM2M	15.0	20.8	10.4	21.8	5.8	6.5	-0.6	4.4	11.4	10.6
INM-CM4	28.5	3.9	35.0	24.9	14.3	2.6	7.9	13.7	13.1	16.0
IPSL-CM5A-LR	39.5	0.3	26.8	32.9	8.9	1.2	4.2	7.5	7.0	14.3
IPSL-CM5A-MR	31.1	5.3	32.3	27.0	10.0	1.9	8.9	10.7	11.1	15.4
IPSL-CM5B-LR	39.7	8.4	41.0	32.0	16.4	0.1	14.7	19.9	19.4	21.3
MIROC5	35.6	7.1	27.9	20.5	15.5	3.2	21.3	23.9	30.7	20.6
MIROC-ESM	31.4	5.0	30.1	18.9	8.3	10.1	7.8	11.9	11.2	15.0

Percent Bias Estimates of the WRF Model

The computation of the WRF model-based percent bias for 2 locations is shown in Table 4. It shows that hourly precipitation simulation by the WRF model underestimates the annual hourly maximum precipitation in comparison to NCDC observations at these locations. These biases are used to adjust the gridded precipitation generated by the WRF model for the period of 1985-2010 over the study area.

Table 4: Estimates of the percent bias (%) of the precipitation annual hourly maximum precipitation of the WRF model for the period of 1985-2010.

Models	Williamsburg	Norfolk Airport	Average
WRF	-21	-13.1	-17.1

Future Prediction of the Annual Maximum Precipitation

The annual daily maximum precipitation for the future period (2016-2099) provides precipitation frequency and magnitude at the Hampton Roads region (Figure 5). The percent bias that is estimated from these models and for locations can be incorporated into design calculations to decrease uncertainty. For this study, we have not included the percent bias for the models in this location.

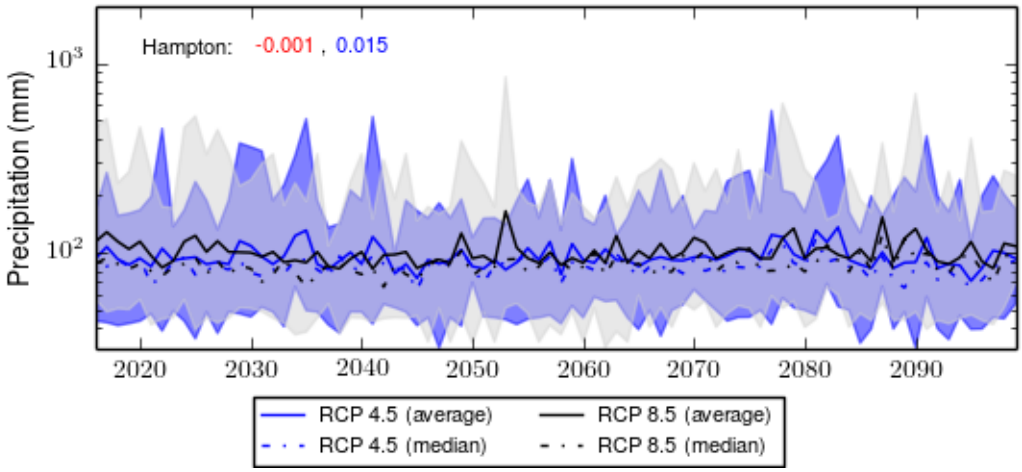

Figure 5: Variability in the future annual daily maximum precipitation for the period of 2016-2099 at Hampton using both RCP4.5 and RCP8.5 scenarios. The grey and blue shaded areas represent the uncertainty predicted by RCP4.5 and RCP8.5 scenarios, respectively.

Spatial Distribution of Annual Daily Maximum Precipitation in the Future

Figures 5 shows the distribution of annual daily maximum precipitation extracted from GFDL-ESM2M precipitation simulation for the period of 2016~2099 over southeastern Virginia. The distribution clearly shows the zones of high and low precipitation. It is also possible to estimate the increase or decrease in precipitation magnitude from these gridded precipitation data for each of the pixels in the domain. Similar to the previous analysis, the percent bias was not included in this distribution, however, with the bias estimates the uncertainty can be reduced.

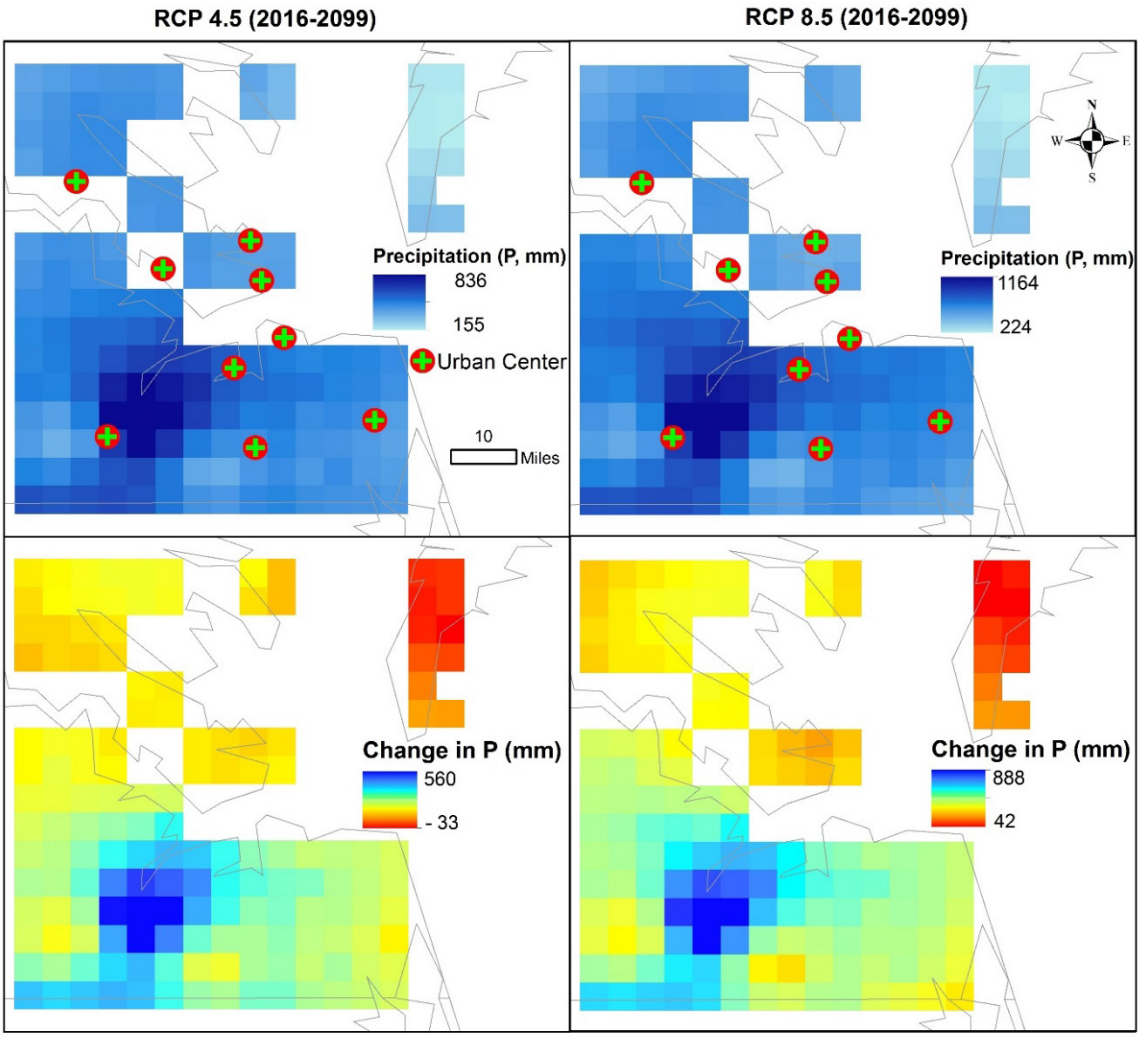

Figure 6: Spatial distribution of future precipitation using RCP scenarios (RCP 4.5, top-left and RCP 8.5, top-right) of the GFDL-ESM-2M model for the period of 2016-2099. The bottom panel represents changes in maximum daily precipitation simulated by the model in the corresponding scenarios.

Conclusions

The analysis of the daily and hourly observations of precipitation at 9 locations in southeastern Virginia provides the foundation for understanding the extreme trends in the region for the period of 1950-2005. However, these estimates are not sufficient to characterize the exact trends in the region. This is due to the fact that either these stations are located outside the urban center, far away from each other, and insufficient quality of the data. In addition, instrumentation and manual intervention often complicate conclusive precipitation characteristics analysis. Besides, the observation data has the limitation of forecasting future scenarios that are necessary for infrastructure design and maintaining human activities.

Gridded precipitation products are developed and used to analyze distributed precipitation characteristics. These products overcome the limitation of *in-situ* observations in many aspects and provide precipitation estimates for areas that lack precipitation estimates. The gridded daily precipitation of the climate models provides geographically a more complete evaluation of the region. The comparison of the annual daily maximum precipitation of the model with NCDC observation provided evidence of bias in the climate models and WRF model outputs that can be integrated in the precipitation estimates to reduce the uncertainty. Similarly, when annual hourly maximum precipitation estimates from the WRF model were compared with NCDC observations, the percent bias derived can be used for the design calculations. However, the reduction in the uncertainty may not be adequate due to the bias correction based on percent bias only from two locations. This uncertainty can be further reduced by comparing precipitation estimates with more *in-situ* observations.

Processed Data Available

Table 5: List of the available data for the precipitation characteristics analysis in southeastern Virginia.

Model/Observation	**NCDC Observation**	**Climate Models (CMIP5- MACA)**		**WRF Model**	
Status		No Bias Correction	No Bias Correction	No Bias Correction	Bias Corrected
Period	1950-2010	1950-2005	2016-2099	1985-2010	1985-2010
Temporal Resolution	Daily /Hourly	Daily	Daily	Hourly	Hourly
Spatial Resolution		$1/16^{th}$ of a degree	$1/16^{th}$ of a degree	$1/16^{th}$ of a degree	$1/16^{th}$ of a degree
Locations/No. of Grid Cells	9 (Daily) 2 (Hourly)	16 x 16	16 x 16	16 x 16	16 x 16

References

Abatzoglou, J. T. (2013). Development of gridded surface meteorological data for ecological applications and modelling. International Journal of Climatology, 33(1), 121-131.

Amengual, A., V. Homar and R. Romero, S. Alonso, C. Ramis 2012:. A Statistical Adjustment of Regional Climate Model Outputs to Local Scales: Application to Platja de Palma, Spain, Journal of Climate, DOI: 10.1175/JCLI-D-10-05024.1

Karl, T. R., and R. W. Knight (1998), Secular trends of precipitation amount, frequency and intensity of the United States, Bull. Am. Meteorol. Soc., 79, 231–241, doi: 10.1175/1520-0477(1998)079<0231: STOPAF>2.0.CO; 2.

Min, S.-K., X. Zhang, F. W. Zwiers, and G. C. Hegerl, (2011), Human contribution to more-intense precipitation extremes, Nature, 470, 378–381.

Osborn, T. J., M. Hulme, P. D. Jones, and T. A. Basnett (2000), Observed trends in the daily intensity of United Kingdom precipitation, Int. J. Climatol., 20, 347–364, doi:10.1002/(SICI)1097-0088(20000330)20:4<347::AID-JOC475>3.0.CO;2-C.

Reichle, R. H., and R. D. Koster, 2004: Bias reduction in short records of satellite soil moisture. Geophys. Res. Lett., 31, L19501, doi:10.1029/2004GL020938.

Sen Roy, S., and R. C. Balling Jr. (2004), Trends in extreme daily precipitation indices in India, Int. J. Climatol., 24, 457–466, doi:10.1002/
joc.995.

Solomon, S., Dahe Qin, Martin Manning, Z. Chen, M. Marquis, K. B. Averyt, M. Tignor, and H. L. Miller. "IPCC, Climate change 2007: the physical science basis. Contribution of working group I to the fourth assessment report of the intergovernmental panel on climate change." (2007): 98-101.

Skamarock, W.C. and Klemp, J.B., 2008. A time-split nonhydrostatic atmospheric model for weather research and forecasting applications.Journal of Computational Physics, 227(7), pp.3465-3485.

Wood, A., L. R. Leung, V. Sridhar, and D. P. Lettenmaier, 2004: Hydrologic implications of dynamical and statistical approaches to downscaling climate outputs. Climatic Change, 62, 189–216.

Effect of rain gauge proximity on rain estimation for problematic urban coastal watersheds in Virginia Beach, VA

Jeffrey M. Sadler[a], Mohamed M. Morsy[a], Jonathan L. Goodall Ph.D., P.E.[c]

[a] *Graduate Research Assistant, Civil and Environmental Engineering, University of Virginia*
[c] *Associate Professor, Civil and Environmental Engineering, University of Virginia*

Contents

List of Figures

List of Tables

Problem

As sea levels rise, coastal cities are becoming increasingly vulnerable to both severe and minor flooding (Nicholls and Cazenave, 2010). Extreme events, such as hurricanes and tropical storms, have caused severe damage, costing major coastal cities billions of dollars and thousands of lives (Kates et al., 2006; Galarneau et al., 2013). In addition to extreme, high return-period events, small return-period rainfall events can also cause flooding in coastal cities. These cities typically have very low topographic relief, a high water table, and tidal influences which combine to make drainage problematic (Titus et al., 1987). The frequency of these lower return period flood occurrences has increased in coastal cities in recent years (Ezer and Atkinson, 2014; Sweet et al., 2014). These flooding events, while less dramatic, nevertheless can have significant economic and social costs (Suarez et al., 2005).

To understand and accurately forecast flooding at the urban watershed scale, spatially and temporally detailed rainfall data are needed (Smith et al., 2007) but usually unavailable (Hill, 2015). The typical urban watershed is small in area and has a large proportion of impervious surfaces. This results in a short runoff response time (Hall, 1984; Fletcher et al., 2013). Typically, neither rain gauge networks nor weather radar can provide rainfall measurements at spatial and temporal resolutions needed to make relevant urban flood forecasts (Hill et al., 2014); the traditional rain gauge networks are typically too coarse spatially to provide such detailed information (Seo, 1998). Weather radar can produce measurements with much higher spatial resolutions; however, weather radar measurements are indirect requiring an empirically-derived relationship between reflectivity from rain clouds and actual rainfall on the ground (Smith and Krajewski, 1993) and are therefore inherently uncertain to some degree. Efforts have been taken to blend the two data sources (Velasco-Forero et al., 2009; Seo, 1998; Sun et al., 2000) but spatially detailed and accurate rainfall data are usually difficult to obtain (Hill et al., 2014). To increase the spatial coverage of rainfall estimation, less traditional technologies such as measuring signal attenuation between cell phone towers (Overeem et al., 2013; Zinevich et al., 2008) and using simple, more widespread binary rainfall sensors (Hill, 2015) have recently been evaluated.

Although it is generally accepted that spatially and temporally dense measurements are needed to capture storm events relevant to urban hydrology, the degree of spatial and temporal density is uncertain. This has been studied using both rain gauge networks (Pedersen et al., 2010; Serinaldi, 2008; Jensen and Pedersen, 2005) and weather radar (Krajewski et al., 2003; Smith et al., 2007). Ciach and Krajewski (2006) used 25 rain gauges stations in a 3km X 3km grid to observe small-scale spatial and temporal rainfall variation. In their findings, rainfall exhibited high spatial variability with correlation coefficients decreasing to below 0.8 between gauges at a four kilometer separation distance at a 15 minute time step; the correlation coefficients were lower at a 5 minute time step. Emmanuel et al. (2012) analyzed rainfall radar images finding rainfall patterns to be very spatially heterogeneous with decorrelation distances as low as 5 km. Berne et al. (2004) used geostatistcs with rain gauge and an X-Band weather radar data to suggest a simple empirical relationship between watershed area and the corresponding necessary temporal resolution (Equation 1); they then related the temporal resolution to the needed spatial resolution (Equation 2).

$$\Delta t = 0.75S0.3 \quad (1)$$

$$\Delta r = 1.5\sqrt{\ }\Delta t \quad (2)$$

Approach

The above studies focused on describing the temporal and spatial characteristics of rainfall in a small-scale or urban context but they did not explore what effect the ability to characterize rainfall events would have on rainfall estimation for urban watersheds. Researchers who have considered the impact of spatial or temporal heterogeneity on watersheds did so on a much larger scale than what is considered here (Maskey et al., 2004; Smith et al., 2007; Segond et al., 2007). The objective of this paper is to better

understand how rain gauge proximity affects rainfall estimation for small (< 1km^2) problematic urban watersheds in Virginia Beach, VA.

Methodology

Study area and focus watersheds

The study area is the more populated portion of the City of Virginia Beach (CVB), Virginia. Virginia Beach is the largest geographically (645 sq. km) and most populous city (pop. 450,980) in the commonwealth of Virginia (US Census). Most of the residents of Virginia Beach live in the northern portion of the city. The study area, shown in Figure 1, is 370 sq. km, 57% of the total city area, and roughly the northern half of the city.

Specific intersections with recurrent flooding problems were provided by city engineers. The drainage area corresponding to each of these points was delineated using a 1 m X 1 m resolution digital elevation model (DEM). The resulting watersheds are shown in Figure 2 and their characteristics are given in Table 1. For each watershed the percent imperviousness was obtained from the National Land Cover Dataset 2011 and the percent slopes were calculated from the DEM.

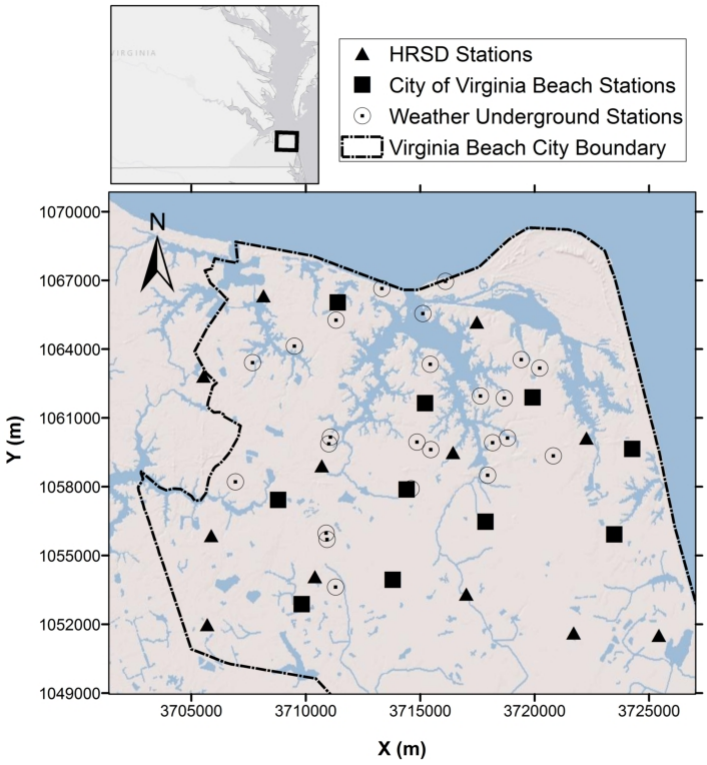

Figure 1: Study area

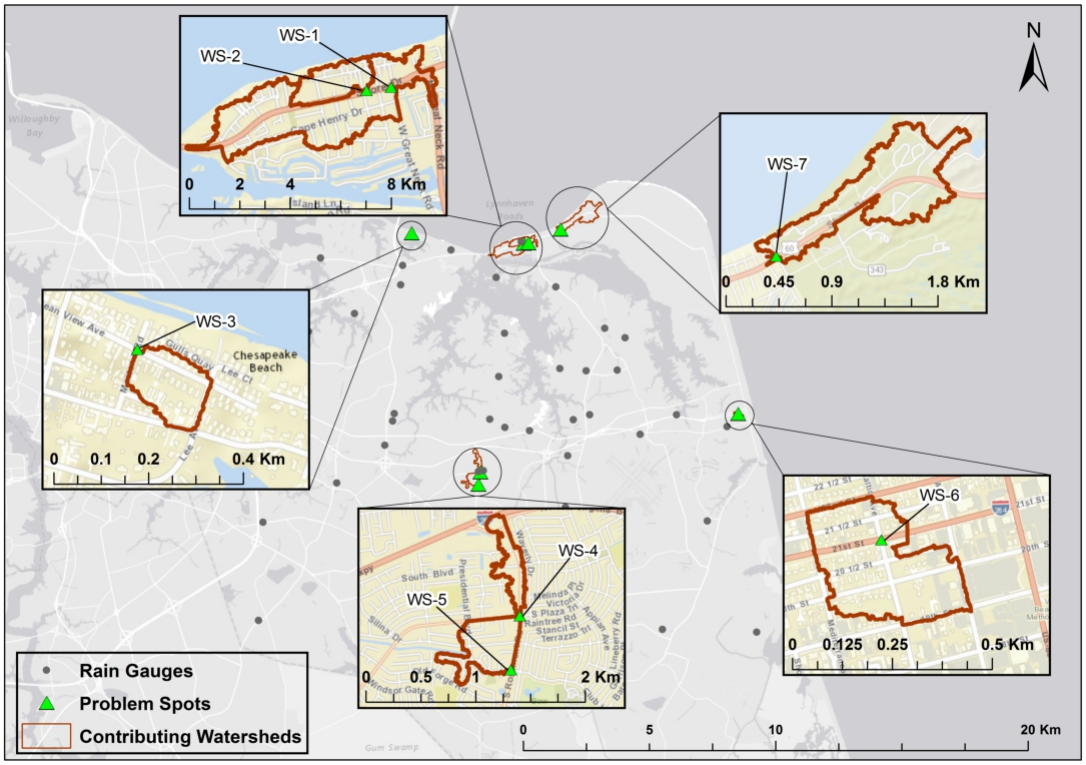

Figure 2: Focus watersheds

Table 1: Focus watershed areas

ID	Description	Area (km2)	% Impervious	Ave. % Slope
WS-1	Shore Drive and Great Neck Road	0.76	59	4.7
WS-2	Shore Drive and Red Tide Road	0.15	69	0.6
WS-3	Ocean View Ave and Mortons Road	0.02	43	5.3
WS-4	S. Rosemont and S. Plaza Trail	0.13	61	3.9
WS-5	S. Rosemont and Clubhouse	0.26	26	4.4
WS-6	21st and Baltic	0.08	46	3.3
WS-7	Shore Drive and Kendall Street	0.69	9	11

Rainfall Data

Precipitation data were obtained from three different sources: The CVB, Hampton Roads Sanitation District (HRSD), and Weather Underground (WU). The 20 dates with the highest daily precipitation measurements from the Oceana Naval Air Station were used in the analysis. Figure 3 shows the total daily rainfall and the standard deviation for the 20 days analyzed.

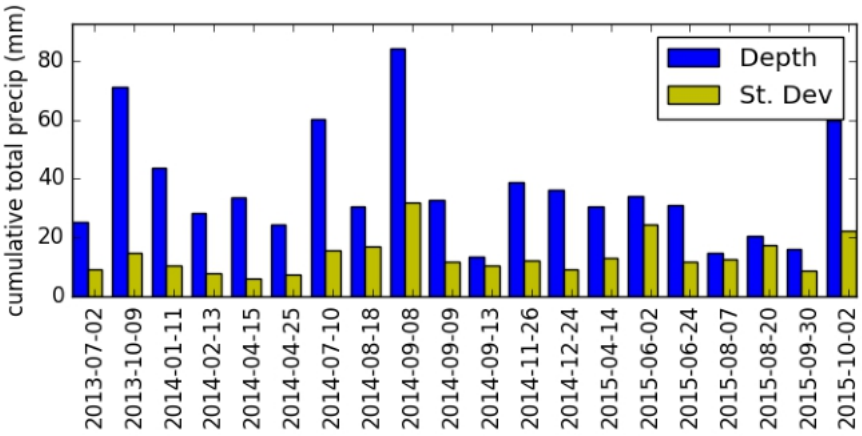

Figure 3: Average daily cumulative rainfall depth and standard deviations of selected days

The city of Virginia Beach in the past five years has installed a rain gauge network consisting of fourteen gauges. Precipitation data from the ten gauges within the study area were obtained for the 20 days analyzed. These data were recorded at five minute intervals.

The HRSD has a network of over 50 rain gauges over the Hampton Roads area, 12 of which are within the study area. The data from these gauges are quality controlled by the HRSD. The measurements were recorded in 15 minute intervals.

Crowd-sourced data were obtained from WU (http://www.wunderground.com/), using their web API. In addition to the 12,000 National Weather Service and Public Stations used by WU, more than 100,000 personal weather stations contribute to the site. These stations are purchased and maintained by individuals. In Virginia Beach for the 20 days examined, there were between 7 and 21 WU personal weather stations that reported rainfall values; that corresponds to a 70-210% increase in the number of gauges in the study area. The temporal resolution amongst these stations was variable with an average of a 6.2 minute measurement interval. Increased spatial coverage has obvious benefits in better understanding spatially heterogeneous precipitation events. However, because the data are crowd-sourced with minimal quality control, their validity is uncertain. The process for screening this dataset to remove invalid observations is described in the following section.

Analysis

Quality Controlling of WU Data

The following procedure was used to quality control the WU rainfall observations. First, if a stations recorded a daily rainfall total of zero for any of the 20 days analyzed, all values from that gauge for that day were disregarded. This assumes that if a gauge does not record any rainfall for one day, that gauge was not working that day. Second, anomalous measurements at the 15 minute time step were tallied as follows. At each WU station, the inverse distance weighting (IDW) method was used to predict the rainfall

based on its neighboring stations maintained by the CVB and the HRSD. A minimum of three stations, and all within 5000 m were used for the estimation. For each 15 minute time step, the IDW-based, estimated value was compared to the value recorded by the WU station. If the predicted value was three or more standard deviations from the recorded value, that measurement was flagged as an outlier. The measurement was also flagged as an outlier if the predicted value was greater than 10 mm and the recorded value was zero. The total percentage of outliers measured at each station was measured. Then the percentage of outliers compared to all measurements at each station was calculated. The process was also performed with the CVB and HRSD stations as well. As a baseline for comparison, the percentage of outliers for the WU stations were compared to those of the CVB and HRSD stations. In this way, unreliable WU stations were identified.

Exploratory Data Analysis

To gain a broad picture of the spatial heterogeneity of the collected rainfall data, rainfall depths for all stations and all time scales (daily, hourly, and 15 minute) were plotted. The standard deviations of the rainfall depths were compared to the mean at daily, hourly, and 15 minute time scales.

Rainfall interpolation using Kriging

Ordinary Kriging was used to quantify the importance of rain gauge proximity in estimating rainfall depth over the seven focus watersheds. It would have preferable to use Kriging with external drift (Kebaili Bargaoui and Chebbi, 2009), however this technique requires another related but independent variable such as elevation (Goovaerts, 2000). In this case, since the study area is located on a coastal plane, the elevation is effectively constant over the study area so Ordinary Kriging was chosen. A spherical model was used for the Kriging semi-variograms. The model parameters (sill and range) were automatically optimized using the RGeostats package in R (Renard et al., 2015). Those parameters were then used in ArcGIS to predict rainfall throughout the study area for each time period.

Rainfall estimation without local information

To quantify the role of local rain gauges in area-averaged precipitation estimates for the seven focus watersheds, the rainfall was estimated with and then without nearby gauging stations. The nearest HRSD or CVB gauge and any nearer WU gauges were considered 'nearby'. The estimated rainfall and variance with nearby stations were computed and averaged over the focus watersheds. These same values were then estimated without the nearby stations and the results were compared to the results of the estimation with the nearby stations. The number of gauges removed for each focus watershed and the average distance of the removed gauges are shown in Table 2.

Rainfall estimation without increasingly distant information

A second analysis was performed to quantify what effect increasing distance to the nearest rain gauge has on rainfall estimation. For each focus watershed, first the nearest rain gauge from the watershed centroid was excluded and the rainfall and variance were estimated. Then the next closest station was excluded as well and the rainfall and variance were again estimated. This pattern was followed until the 12 nearest rain gauges to the watershed centroid were excluded. The incremental change in the rainfall estimation and variance compared to the distance of the furthest excluded rain gauge was plotted.

Table 2: Gauges removed in Kriging analysis

Area (km^2)	Num. gauges removed	Min. distance of removed gauges (m)
0.76	3	318
0.15	3	153
0.02	1	1266
0.13	2	458
0.26	2	380
0.08	1	625
0.69	2	2645

Findings

Quality Control Results

The results of the quality control procedure of the WU stations are shown in Figure 4. Eight of the top ten stations in terms of percentage of outliers were WU stations. The WU stations had a higher average percentage of outliers overall (Table 3). Only one stood out statistically: "KVAVIRGI52", which was 3.6 standard deviations from the mean percent number of observations classified as outliers. This station therefore was excluded from the analysis, but all other stations were kept.

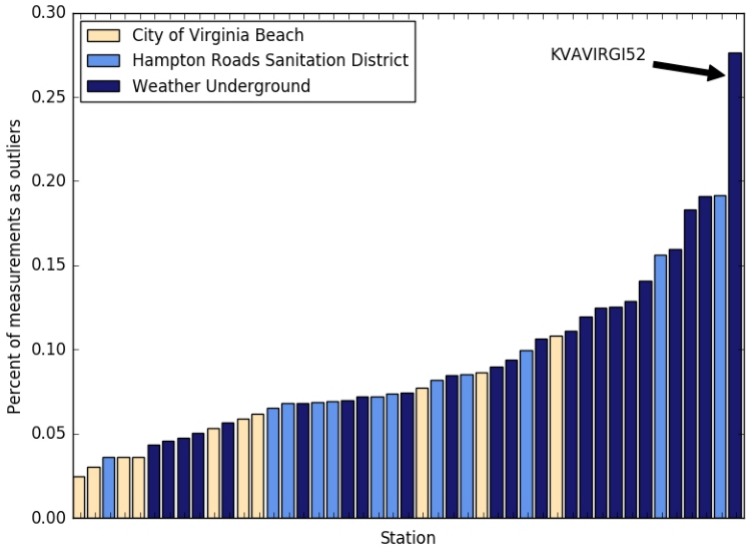

Figure 4: Percent of o

Table 3: Percentage of outliers for each data source

Data Source	Average Percentage of Outliers (%)
CVB	4.5
HRSD	6.9
WU	8.6

Exploratory Analysis Results

Figure 5 shows the daily rainfall depths for each station across the study area. There are clear differences in rainfall magnitude and spatial variation between dates. For example, considering the four daily total rainfall for the dates in the third row of Figure 5 (2014-12-24, 2015-04-14, 2015-06-02, 2015-06-24), it is clear visually that the daily rainfall on 2015-06-02 is more spatially heterogeneous than the other dates. The data in Table 5 confirms this quantitatively. The four daily totals were quite similar: 36.2, 32.6, 34.3, and 31.8 mm respectively. However, their standard deviations are quite dissimilar: the standard deviation for 2015-06-02 is 23.9 mm while the next highest is 11.0 mm on 2015-04-14, less than half. The spatial variation seen visually in Figure 5 may best be explained quantitatively with the standard deviation to mean ratio, or coefficient of variation (CV). Contrasting the plots of two dates with the lowest CV, 2014-04-15 (0.18), and the highest CV, 2015-08-20 (0.85) (Table 5), the spatial uniformity on 2014-04-15 and the spatial non-uniformity on 2015-08-20 are clearly seen.

Although for a daily time step the rainfall can be quite spatially uniform, when considering a shorter time step, the spatial variation often is much higher; the CV for the 15 minute and hourly time steps was on average at least four times the CV of the daily time step (Table 4). Even the date with the smallest CV for the daily time step, 2014-04-15 (0.18), shows quite variable rainfall amounts across stations (CV up to 0.65 at 11:15:00) when considering the 15-min time step (Figure 6). This variability on smaller time steps is important to consider in an urban environment where highly impervious watershed response times are often less than one hour. The uncertainty caused by this variation can result in inaccurate predictions which would cost convenience if false-positive and potentially safety if false-negative.

Table 4: Average CV for the time steps examined

Time scale	Average CV
15 minute	2.1
Hourly	2.0
Daily	0.5

Rainfall estimation without local information

The results of the rainfall estimation without local information are summarized in Figure 7 and 8. These figures explain the significant role that the local gauging stations had on the rainfall estimation. 7 shows the average increase in variance that occurs in each watershed when the nearby gauging stations are excluded from the rainfall estimation. For most of the watersheds, the variance increases by more than 100% and generally, the increase corresponds to the distance from the watershed centroid to the nearest excluded gauge (see 2). These values vary little between time steps. The variance is a measurement of uncertainty and is related to the magnitude of the rainfall estimation. Therefore, since the variance magnitude relates to the magnitude of the rainfall estimation, it follows that the percent increase will be very similar across time steps.

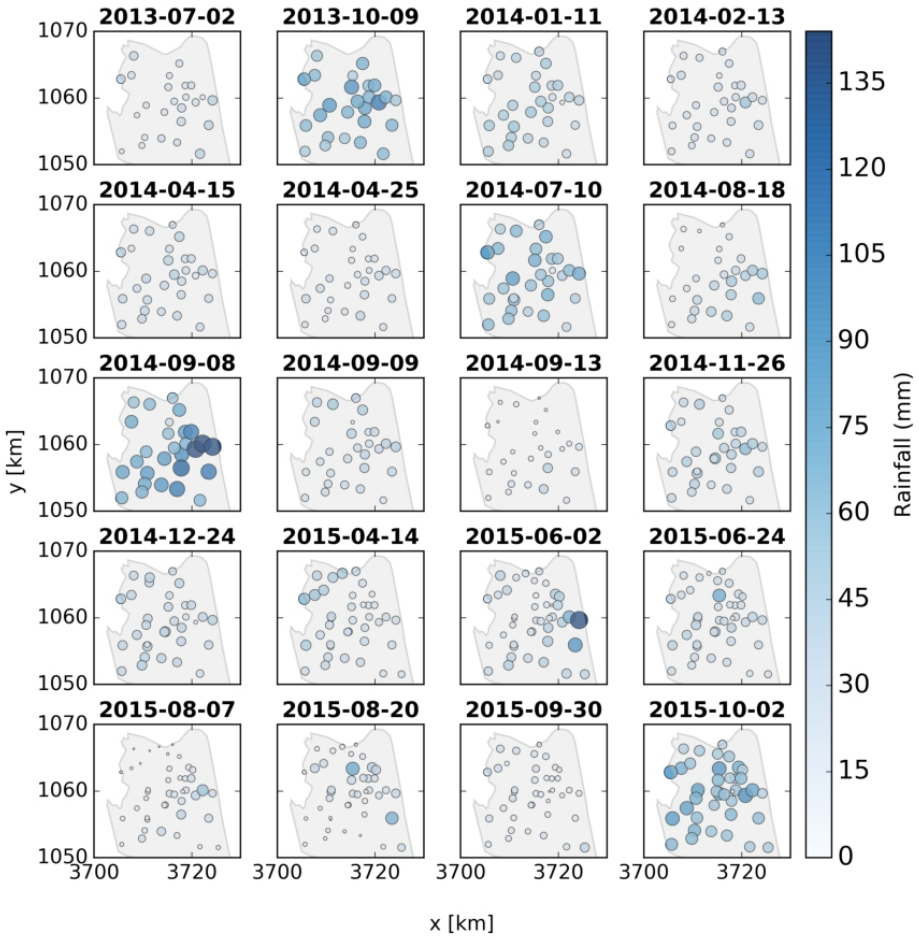

Figure 5: Daily rainfall values at each station

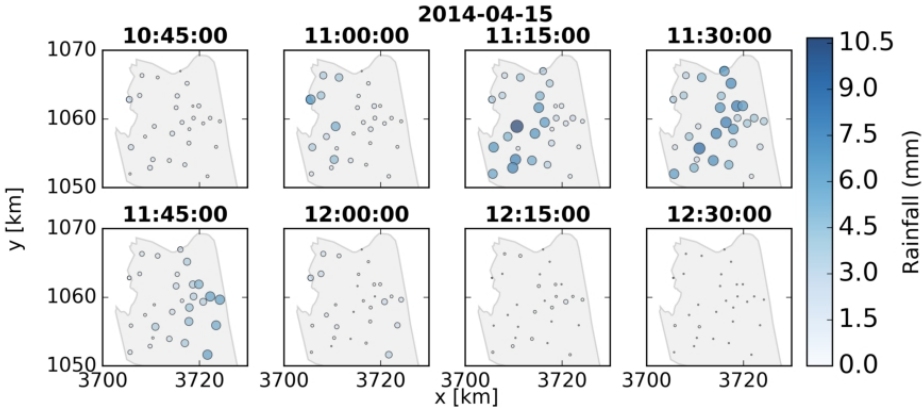

Figure 6: Rainfall values at 15-min time step for 2014-04-15 a storm with low spatial variability on a daily time step

Table 5: Summary data for daily rainfall

Date	Mean (mm)	Standard Dev. (mm)	CV
7/2/2013	25.1	9.2	0.36
10/9/2013	68.8	19.9	0.29
1/11/2014	43.7	10.1	0.23
2/13/2014	28	7.7	0.28
4/15/2014	33.5	6.1	0.18
4/25/2014	24.2	7.1	0.29
7/10/2014	58.5	18.1	0.31
8/18/2014	31.6	16.3	0.51
9/8/2014	84.7	30.9	0.36
9/9/2014	33.1	10.5	0.32
9/13/2014	13.8	10.1	0.73
11/26/2014	39.3	10.6	0.27
12/24/2014	36.2	8.9	0.25
4/14/2015	32.6	11	0.34
6/2/2015	34.3	23.9	0.7
6/24/2015	31.8	10.8	0.34
8/7/2015	15	12.4	0.82
8/20/2015	20.4	17.3	0.85
9/30/2015	17.8	6.9	0.39
10/2/2015	61.5	19.8	0.32

Figure 8 shows the average absolute difference in rainfall estimation when the nearby stations are excluded. On average the percent difference in rainfall estimation for the 15 minute time step was 49% with a maximum of 72% for WS-2. The average absolute difference in rainfall estimation was 0.34 mm. The maximum difference in rainfall estimation was 24.5 mm at WS-6. The intensity of this 15 minute time period (98mm/hr) closely corresponds to a 2-year design storm of the neighboring city of Norfolk (corresponding information for Virginia Beach was not provided). This illustrates the need for local information. The rain gauging station excluded from the analysis in this case was 625m from the centroid of WS-6 and the difference for that one 15 minute time step was the difference between estimating a 2-year storm intensity and not. This is a significant difference and would almost certainly affect the in flood forecasting for this area.

Rainfall estimation without increasingly distant information

Figures 9 and 10 show how the variance and estimated rainfall vary with increasing distance to the excluded stations. The greatest change in these results occurs within 1k m. In Figure 9, each of the points with the maximum distance of the removed gauges of less than 1 km had a percent change in rainfall between 20 and 60%. This result suggests that rainfall measurements within 1 km can make a significant difference in areal rainfall estimation. The scatter points generally trend downward as stations further away from the watershed centroid have a smaller percent impact on the areal rainfall estimation. In a similar, but more definite way, Figure 10 shows how variance changes with increasing the distance of removed stations. The variance decreases drastically as the maximum distance of removed gauges increases from 0 to 1.5 km and is effectively negligible by 3.5 m. Therefore, in this study area, on

average, to appreciably increase the certainty of rainfall estimation, a new rain gauge must be within 3.5 km and would preferably be within 1 km.

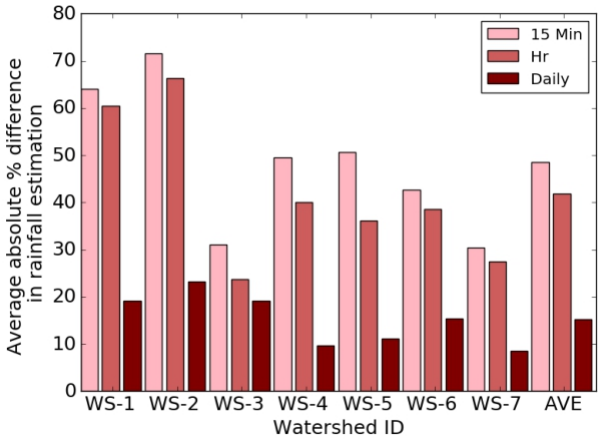

Figure 7: Average percent increase in variance without 'local' data

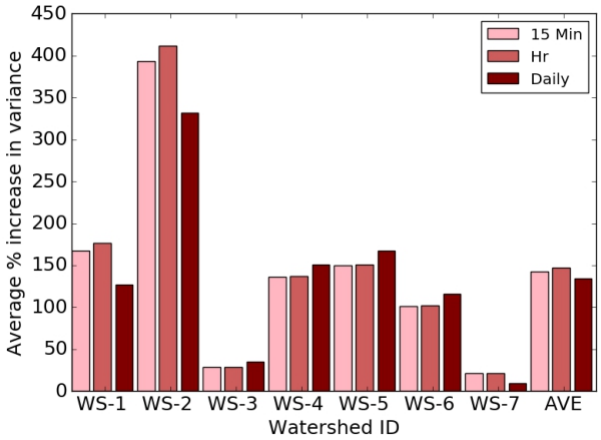

Figure 8: Average percent difference in rainfall estimation from Kriging without 'local' data

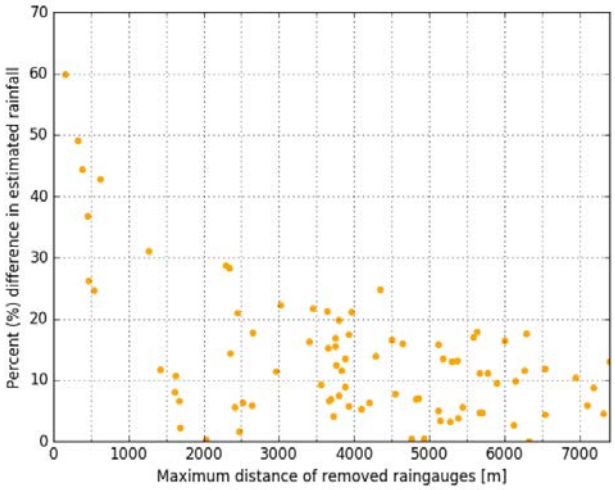

Figure 9: Percent change in variance and percent difference in rainfall estimations compared to distance from watershed centroid to excluded measurement stations at 15-minute time scale

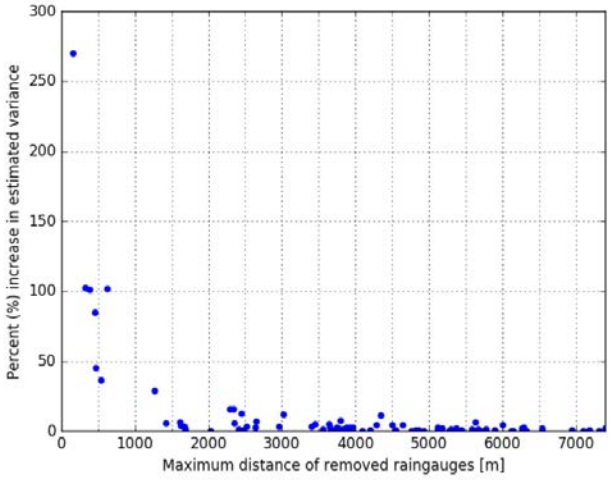

Figure 10. Percent change in variance and percent difference in rainfall estimations compared to distance from watershed centroid to excluded measurement stations at 15-minute time scale

Conclusions

The objective of this research was to quantify how the proximity of rain gauges to problem watersheds in Virginia Beach, VA impacted the areal-average rainfall estimated for the watersheds. Rainfall data from three different sources, the City of Virginia Beach, the Hampton Roads Sanitation District, and Weather Underground, were used for the analysis. The rainfall data used were from the 20 days over a 3 year period with the highest rainfall totals. In total, 44 rain gauges were used in the analysis. The WU data were quality controlled on a station-by-station basis resulting in one station being excluded from the analysis. Kriging was performed to quantify the effect of nearby stations on the rainfall estimation for seven problem watersheds. The results indicated that rainfall estimations changed on average by about 50% across all the watersheds at a 15-minute time scale when the nearby stations were excluded. For one of the watersheds, the highest average change in rainfall estimation was above 70% at a 15-minute time step and the largest difference in rainfall estimation was 24.5 mm over 15 minutes. Differences of this magnitude at a 15-minute time scale could drastically affect flood forecasts for these small, flashy, urban watersheds. Analysis was also performed to assess the effect on rainfall estimation from increasingly distant rain gauges from the watershed centroid. The results of this analysis suggest that a rain gauge should be within 1 km and preferable within 500 m of the centroid of a problem watershed in order to accurately predict rainfall falling within that watershed on a 15-minute time step. While the research in this paper was specific to Virginia Beach, the results may have application to watersheds in other cities with similar climatic and geographic characteristics.

Recommendations

In the study area, to best capture rainfall on a 15-minute time step, it is recommended that a rain gauge should be placed within 500 m of the flood prone area. Rain gauges greater than 1 km from the problem area may not accurately represent the true rain falling at that area on a 15-minute time step. This could lead to inaccurate forecasts within flood warning applications.